HHS Public Access

Author manuscript

J Immunol. Author manuscript; available in PMC 2017 February 15.

Published in final edited form as:

J Immunol. 2016 February 15; 196(4): 1891–1899. doi:10.4049/jimmunol.1501555.

p52 over-expression increases epithelial apoptosis, enhances lung injury, and reduces survival after LPS treatment[1]

Jamie A. Saxon[*], **Dong-Sheng Cheng**[†], **Wei Han**[†], **Vasiliy V. Polosukhin**[†], **Allyson G. McLoed**[*], **Bradley W. Richmond**[†,§], **Linda A. Gleaves**[†], **Harikrishna Tanjore**[†], **Taylor P. Sherrill**[†], **Whitney Barham**[*], **Fiona E. Yull**[*], and **Timothy S. Blackwell**[*,†,‡,§]

[*]Department of Cancer Biology, Vanderbilt University, Nashville, TN, USA, 37232

[†]Division of Allergy, Pulmonary and Critical Care Medicine, Department of Medicine, Vanderbilt University, Nashville, TN, USA, 37232

[‡]Department of Veterans Affairs Medical Center, Nashville, TN 37232

[§]Department of Cell and Developmental Biology, Vanderbilt University, Nashville, TN, USA, 37232

Abstract

While numerous studies have demonstrated a critical role for canonical NF-κB signaling in inflammation and disease, the function of the non-canonical NF-κB pathway remains ill-defined. In lung tissue from patients with acute respiratory distress syndrome (ARDS), we identified increased expression of the non-canonical pathway component p100/p52. To investigate the effects of p52 expression *in vivo*, we generated a novel transgenic mouse model with inducible expression of p52 in Clara cell secretory protein (CCSP)-expressing airway epithelial cells. While p52 over-expression alone did not cause significant inflammation, p52 over-expression caused increased lung inflammation, injury, and mortality following intratracheal delivery of *Escherichia coli* LPS. No differences in cytokine/chemokine expression were measured between p52 over-expressing mice and controls, but increased apoptosis of CCSP+ airway epithelial cells was observed in transgenic mice after LPS stimulation. *In vitro* studies in lung epithelial cells showed that p52 over-expression reduced cell survival and increased expression of several pro-apoptotic genes during cellular stress. Collectively, these studies demonstrate a novel role for p52 in cell survival/apoptosis of airway epithelial cells and implicate non-canonical NF-κB signaling in the pathogenesis of ARDS.

INTRODUCTION

NF-κB regulates a number of key genes involved in cellular processes such as proliferation, apoptosis, and inflammation. The NF-κB transcription factor family contains 5 members (p65/RelA, p100/p52, p105/p50, RelB, and c-Rel). Traditionally, NF-κB signaling is

[1]This work was supported by the National Institutes of Health (NHLBI HL092870, HL085317) and the Department of Veterans Affairs (Merit Review Award 1l01BX002378).

[2]Address correspondence to Dr. Timothy S. Blackwell, Vanderbilt University School of Medicine, 1161 21st Avenue South, T-1218 MCN, Nashville, TN 37232. Phone: 615-343-4761, Fax: 615-322-2582, timothy.blackwell@vanderbilt.edu.

associated with activation through either the canonical or non-canonical signaling pathways. In the non-canonical pathway, a heterodimer consisting of p100 and most commonly RelB remains sequestered in the cytoplasm due to the IκB-like inhibitory C-terminus of p100. Upon activation, p100 is phosphorylated and undergoes partial proteolytic processing to p52, enabling the p52-containing heterodimer to translocate into the nucleus. While many studies have identified crucial roles for canonical NF-κB signaling in inflammatory diseases, metabolic disorders, and cancer, few have investigated the involvement of non-canonical NF-κB signaling in these contexts. Global knockout of either *Relb* or *Nfkb2* (the genes for RelB and p100/p52) causes defects in secondary lymphoid organ development and impaired immune responses (1–3). Therefore, non-canonical NF-κB signaling has primarily been studied in hematopoietic cells, where it is an important pathway for regulating chemokine genes required for normal lymphoid organ development (4, 5). However, little is known about the function of non-canonical NF-κB signaling in non-immune cell types.

Acute respiratory distress syndrome (ARDS)[3] is a life-threatening form of hypoxemic respiratory failure that results in substantial morbidity and mortality. ARDS is characterized by an influx of inflammatory cells, epithelial apoptosis, and vascular permeability. Intratracheal (IT)[4] treatment of mice with *Escherichia coli* LPS is commonly used as a model of ARDS. We have previously shown that NF-κB signaling in the lung epithelium regulates the inflammatory response after LPS stimulation (6), suggesting that epithelial NF-κB signaling is a critical component of ARDS pathogenesis. Although the role of the non-canonical NF-κB pathway in LPS-induced inflammation is unknown, studies with lung epithelial cells *in vitro* have shown that LPS stimulation induces non-canonical NF-κB activation with slower and more protracted kinetics compared to canonical NF-κB activation and that non-canonical NF-κB signaling may be important for regulation of pro-inflammatory cytokines (7).

To study the effects of non-canonical NF-κB signaling *in vivo*, we generated a novel transgenic mouse model with inducible expression of p52 specifically in airway epithelial cells. We found that p52 over-expression alone did not affect inflammatory cell recruitment or signaling; however, p52 over-expression in conjunction with LPS stimulation led to increased mortality, exaggerated lung injury, and enhanced epithelial cell apoptosis. Together, these studies demonstrate a novel role for non-canonical NF-κB signaling in cell survival/apoptosis during cellular stress and implicate p52 as a factor affecting the severity of ARDS pathogenesis.

MATERIALS AND METHODS

Generation of CCSP-p52 mouse model

The p52 cFlag pcDNA3 plasmid containing C-terminal FLAG-tagged murine p52 was a gift from Stephen Smale (Addgene plasmid #20019). This plasmid was digested first with HindIII followed by SacI digestion to obtain a fragment containing the FLAG-p52. The ends of this fragment were filled in before ligation into the EcoRV site of a modified pBluescript

[3]ARDS, Acute Respiratory Distress Syndrome
[4]IT, intratracheal

II SK expression vector, which contains a (tet-O)$_7$-CMV promoter consisting of seven copies of the tetracycline (tet)[5] operator DNA-binding sequence linked to a minimal CMV promoter together with bovine growth hormone poly-adenylation sequences to ensure transcript termination. The final plasmid ((tet-O)$_7$-FLAG-p52-BGH.poly(A)) was verified by sequencing. To prevent basal leakiness, a construct expressing a tetracycline-controlled transcriptional silencer (tTS)[6] under control of the Clara cell secretory protein (CCSP)[7] promoter (CCSP-tTS-hGH.poly(A)) was also included (6, 8). The (tet-O)$_7$-FLAG-p52 microinjection fragment was excised from the plasmid by digesting with AscI, resulting in a 2.1 kb fragment. The 5 kb CCSP-tTs fragment was excised using XhoI and NotI. Both constructs were purified with the GELase Agarose Gel-Digesting Preparation kit (Epicentre) following the manufacturer's instructions. These constructs were co-injected at the Vanderbilt Transgenic Mouse/Embryonic Stem Cell Shared Resource to generate transgenic lines of FVB background mice with co-integration of both the CCSP-tTS and the (tet-O)$_7$-FLAG-p52 transgenes. Genotyping of the founder animals was performed by Southern blot, and all subsequent genotyping was performed by PCR analysis. Primers used for PCR of the (tet-O)$_7$-p52-FLAG are as follows: F: GACGCCATCCACGCTGTTTTG and R: AGGATAGGTCTTCCGGCCCTT. The product size is 322 bp. Primers used for PCR of the CCSP-tTS are as follows: F: GAGTTGGCAGCAGTTTCTCC and R: GAGCACAGCCACATCTTCAA. The product size is 472 bp. Four founder lines of CCSP-tTS/(tet-O)$_7$-FLAG-p52 mice were mated with CCSP-rtTA[8] homozygous mice (gift from Dr. J.A. Whitsett, University of Cincinnati, Cincinnati, OH) (9) to obtain triple transgenic mice, which were designated CCSP-p52[9]. CCSP-p52 mice generated from two separate founder lines of CCSP-tTS/(tet-O)$_7$-FLAG-p52 mice were used for these studies.

Animal experiments

All animal care and experimental procedures were approved and conducted according to the guidelines of the Vanderbilt University Institutional Animal Care and Use Committee. For experiments, age- and sex-matched mice were administered 2 g/l doxycycline (dox)[10] in 2% sucrose drinking water to activate transgene expression. Water was replaced twice weekly. Mice were sacrificed at indicated time points, and genotype-negative littermates (designated WT[11]) were used as controls. Lungs were lavaged as previously described (10), and the left lung was tied off and flash-frozen in liquid nitrogen. The right lung was perfused and fixed by inflating with 10% neutral-buffered formalin. Total and differential bronchoalveolar lavage (BAL)[12] cell counts were determined as previously described (11).

LPS, bleomycin, and RelB adenovirus administration

To establish transgene expression, mice were placed on dox for 1 week prior to IT LPS, bleomycin, or RelB adenovirus administration, and they remained on dox until sacrifice. For

[5] tet, tetracycline
[6] tTS, tetracycline-controlled transcriptional silencer
[7] CCSP, Clara cell secretory protein
[8] rtTA, reverse tetracycline-transactivator
[9] CCSP-p52; CCSP-rtTA (tet-O)$_7$-FLAG-p52 mice
[10] dox, doxycycline
[11] WT, wild-type
[12] BAL, bronchoalveolar lavage

IT treatments, mice were anesthetized with isofluorane. *Escherichia coli* LPS (serotype 055:B5; Sigma-Aldrich) was diluted in sterile PBS and delivered IT at a dose of 3 μg/g body weight. Bleomycin (0.08 units) diluted in sterile saline was administered IT. 5×10^8 pfu of RelB-His adenovirus containing murine RelB with a His tag (Ad-RelB[13]; ABM) or control luciferase adenovirus (Ad-Luc[14]; gift from Dr. A. Powers, Vanderbilt University, Nashville, TN) was delivered IT. Inflammatory cell recruitment was assessed 96 hours after adenoviral administration. For experiments with LPS stimulation after adenovirus administration, LPS was given IT 96 hours after adenoviral delivery.

Lung histology

H&E staining was performed on 5 μm lung sections to assess lung histology. A pathologist scored lung fibrosis on H&E-stained sections as previously described using a 0 to 4 point scale (0 = normal lung architecture; 1 = increased thickness of ≤50% of interalveolar septa; 2 = thickening of >50% of interalveolar septa without fibrotic foci formation; 3 = thickening of the interalveolar septa with isolated fibrotic foci formation; 4 = formation of multiple fibrotic foci with distortion of parenchymal architecture) (12).

Immunostaining

To evaluate transgene expression in CCSP-p52 mice, 5 μm lung sections were stained with an anti-FLAG antibody (600-403-383, Rockland). For TUNEL immunofluorescence staining, lung sections were stained using the fluorescein *In Situ* Cell Death Detection Kit (Roche), and TUNEL positive cells were counted in fifteen 60x fields using fluorescent confocal microscopy. Mean scores were calculated for each animal. For TUNEL co-immunofluorescence staining with CCSP or surfactant protein C (SPC)[15], lung sections were first stained with anti-CCSP (S-20; Santa Cruz) or anti-SPC antibody (Millipore) followed by the TUNEL staining protocol. SPC and TUNEL double-positive cells were enumerated in ten 20x fields, and total CCSP and TUNEL double-positive cells were counted on each lung section using fluorescent confocal microscopy. To assess nuclear p52 in human lungs, immunostaining using an anti-p52 antibody (C-5, Santa Cruz) was performed on normal lung sections from 4 life-long non-smokers and on lung sections from 4 patients with ARDS. ARDS lung sections were a generous contribution from Dr. Lorraine Ware (Vanderbilt University, Nashville, TN). All patients had no known chronic lung disease.

Generation of p52-overexpressing RLE-6TN cells

Rat type II alveolar epithelial cell line RLE-6TN (ATCC) was maintained at 37°C 5% CO_2 in DMEM (Invitrogen) with 4.5 g/l glucose and 2 mM L-glutamine, supplemented with 10% fetal bovine serum, 100 units/ml penicillin, and 100 μg/ml streptomycin. p52 expression construct p52 cFLAG pcDNA3 and control empty vector cFLAG pcDNA3 were gifts from Stephen Smale (Addgene plasmids #20019 and #20011). RLE-6TN (RLE-WT)[16] cells were

[13]Ad-RelB, adenoviral RelB
[14]Ad-Luc, adenoviral luciferase
[15]SPC, surfactant protein C
[16]RLE-WT, RLE-6TN parental cells

transfected with p52 cFLAG pcDNA3 or empty vector cFLAG pcDNA3 using Effectene transfection reagents (Qiagen) according to the manufacturer's protocol, and G418-selected clones were pooled. To confirm transgene expression, the NE-PER Nuclear and Cytoplasmic Extraction Reagents (Thermo Scientific) were used to prepare nuclear protein from parental empty vector (RLE-EV)[17] and p52 cFLAG (RLE-p52)[18] transfected cells that had undergone selection, and a Western blot was performed and probed with antibodies as described for Western blot analysis below.

Cell viability measurements

Cell viability of parental (RLE-WT), empty vector (RLE-EV), and p52-overexpressing (RLE-p52) RLE-6TN cells was assessed using the CellTiter-Glo Luminescent Cell Viability assay (Promega) according to the manufacturer's protocol. For serum starvation experiments, an equal number of RLE-WT, RLE-EV, and RLE-p52 cells were plated in 96 well plates in 10% serum medium as described above. Eight hours later, when cells had adhered to the wells, cells were switched to medium lacking serum, and cell viability was assessed after 12, 18, and 24 hours in medium without serum. Percent survival was determined by normalizing no serum viability measurements to viability measurements in 10% serum medium for each cell line at each time point. For H_2O_2 treatment experiments, an equal number of RLE-EV and RLE-p52 cells were plated in 96 well plates. After overnight incubation, cells were treated with 100 μM H_2O_2, and cell viability was assessed at 24 hours. Percent survival was determined by normalizing H_2O_2-treated viability measurements to viability measurements in control (untreated) cells.

Western blot analysis

Nuclear protein was prepared from lung tissue and RLE-6TN cells using the NE-PER Nuclear and Cytoplasmic Extraction Reagents (Thermo Scientific), separated by SDS-PAGE gel, transferred to nitrocellulose membranes, and probed using the following antibodies: FLAG (F3165, Sigma), p100/p52 (4882, Cell Signaling), p65 (C-20, Santa Cruz), p50 (C-19, Santa Cruz), RelB (C-19, Santa Cruz), cRel (C, Santa Cruz), and TATA-binding protein (TBP)[19] (N-12, Santa Cruz). Whole cell lysates were prepared from RLE-6TN cells using RIPA buffer (Invitrogen) and probed with antibodies for caspase-3 (9662, Cell Signaling) and actin (AC-74, Sigma). Immunodetection was performed using the corresponding AlexaFluor-conjugated antibodies and the Odyssey Infrared Imaging System (LI-COR Biosciences). All images were converted to grayscale.

Quantitative real-time PCR

Total mRNA was isolated using the RNeasy Mini kit (Qiagen) according to the manufacturer's instructions. Quantitative real-time PCR was performed using Sybr Green PCR Master Mix (Applied Biosystems) and the following primer sets: Cxcl12 (F: CCCATTCTCCTCATCCTCAT; R: ACTCTGCTCTGGTGGAAGGT) (13), Cxcl13 (F: AACTCCACCTCCAGGCAGAATG; R: TGTGTAATGGGCTTCCAGAATACC) (14),

[17]RLE-EV, RLE-6TN cells stably transfected with cFLAG pcDNA3
[18]RLE-p52, RLE-6TN cells stably transfected with p52 cFLAG pcDNA3
[19]TBP, TATA box binding protein

Ccl19 (F: GGCCTGCCTCAGATTATCTGCCAT; R: GGAAGGCTTTCACGATGTTCC), Ccl21 (F: GGACCCAAGGCAGTGATGGAG; R: CTTCCTCAGGGTTTGCACATAG) (15), RelB (F: GGGCATCCAGTGTGTTAGGAAGAA; R: GGAAGCAGATCCTGACGACATTCA), and GAPDH (F: TGAGGACCAGGTTGTCTCCT; R: CCCTGTTGCTGTAGCCGTAT). Expression values were normalized to GAPDH using the ΔCT method. For the quantitative real-time PCR array analysis, RLE-WT, RLE-EV, and RLE-p52 cells plated in 10 cm plates underwent serum starvation for 18 hours as described for cell viability measurements. RNA was isolated from cells using the RNeasy Mini Kit (Qiagen) according to the manufacturer's protocol. RNA was converted to cDNA using the RT^2 First Strand Synthesis Kit (Qiagen). Apoptosis genes were assessed using the Rat Apoptosis RT^2 Profiler PCR array (Qiagen) according to the manufacturer's instructions. Four biological replicates were run for each cell type, and threshold cycle values greater than 32 were discarded from the analysis. Expression values for each sample were normalized to the mean of 5 measured housekeeping genes using the ΔCT method.

Multiplex Cytokine Bead Array

Levels of IFNγ, IL-1β, MCP-1, G-CSF, IL-6, KC, and MIP-1α were measured in BAL fluid and lung lysates as part of a multiplex mouse cytokine magnetic bead array panel (EMD Millipore, Darmstadt, Germany) using a Luminex 100 analyzer. Assays were performed according to the manufacturer's instructions with assistance from the VUMC Hormone Assay and Analytical Services Core. Other analytes in the panel that were below the limit of detection include GM-CSF, IL-4, IL-10, and IL-12p40.

ELISAs

Lung nuclear protein was isolated as described for Western blot analysis, and p52 was detected using the TransAM NF-κB ELISA kit (Active Motif). Albumin was measured in cell-free BAL supernatants using the mouse albumin ELISA from GenWay Biotech, Inc. G-CSF, Mip-1α, KC, (R&D Systems) MCP-1, IL-1β, and IFNγ (Biolegend) were measured in whole lung lysates. All ELISAs were performed according to manufacturer's instructions.

Statistics

Data were analyzed using GraphPad Prism 5.0 software (GraphPad Software, Inc.), and all values are presented as the mean ± SEM. Unpaired Student's t-tests were performed for comparisons between two groups. To analyze differences among more than two groups, one-way ANOVA followed by a Tukey's post-test was used. For the Kaplan-Meyer survival analysis, a log-rank test was employed. $p \leq 0.05$ was considered statistically significant.

RESULTS

Increased nuclear p52 accumulation in lungs of ARDS patients

To investigate whether non-canonical NF- κB signaling is activated in the lungs of ARDS patients, we performed p100/p52 immunostaining on lung sections from patients with ARDS and control subjects. Faint cytoplasmic staining but no nuclear staining was observed in airways from normal lungs (Fig. 1A, B). In contrast, ARDS airways and parenchyma had

a marked increase in nuclear as well as cytoplasmic staining (Fig. 1A, B). This finding of increased nuclear p52 staining in airways and lung parenchyma of ARDS patients suggests that p52 activation could influence ARDS pathogenesis.

Construction of transgenic mice with inducible expression of p52 in airway epithelium

In order to investigate the role of p52 activation in ARDS, we developed a novel mouse model of p52 expression in the airway epithelium using the tet-on system, placing a C-terminal FLAG-tagged p52 under the control of a $(tet\text{-}O)_7$-CMV promoter. Four founder lines were generated and mated to transgenic mice expressing rtTA under the control of the airway epithelial-specific CCSP promoter, generating mice designated CCSP-p52.

To test the induction of p52 expression, CCSP-p52 mice were administered dox in drinking water (2 g/l) for one week. High levels of FLAG-p52 expression were detected in two lines of CCSP-p52 mice by Western blotting of lung nuclear protein (Fig. 2A), demonstrating successful induction of FLAG-p52 expression and translocation of transgenic p52 into the nucleus. FLAG-p52 expression was also detectable in CCSP-p52 mice administered dox for one month (data not shown). No leaky FLAG-p52 expression was detected in other organs after dox treatment or in the lungs in the absence of dox (data not shown). FLAG immunostaining demonstrated FLAG-p52 expression in airway epithelium (Fig. 2B). Together, these data show that CCSP-p52 mice administered dox express p52 in airway epithelium and that transgene expression results in nuclear p52 accumulation.

p52 over-expression in airway epithelium does not significantly alter inflammatory signaling

We investigated whether p52 over-expression *in vivo* results in an inflammatory phenotype similar to canonical NF-κB pathway activation (6). However, no significant difference in inflammatory cells was observed in lungs of CCSP-p52 mice compared to wild-type (WT) mice, and mice exhibited normal lung histology after dox treatment for 1 week or 1 month (Fig. 2D, E). We also measured activation of other NF-κB family members by Western blot using lung nuclear protein extracts from mice on dox for 1 week. As shown in Fig. 2C, no difference was found in activation of other NF-κB family members. These data suggest that p52 over-expression in epithelial cells alone does not alter inflammatory signaling or inflammatory cell recruitment.

CCSP-p52 mice exhibit exaggerated inflammation, lung injury, and mortality after IT LPS

In contrast to canonical NF-κB signaling, which is increased in the lungs within the first 24 hours following IT injection of *Escherichia coli* LPS (16), we found that treatment of WT mice with IT LPS (3 μg/g body weight) leads to increased nuclear p52 in the lungs that peaks at 48 hours (Supplementary Fig. 1). To investigate the function of p52 in the context of LPS stimulation *in vivo*, IT LPS was administered to dox-treated CCSP-p52 and WT mice. A significant increase in mortality was observed in CCSP-p52 mice compared to WT mice beginning 72 hours after LPS (Fig. 3A). We measured albumin in bronchoalveolar lavage (BAL) fluid as a marker of lung injury and found that albumin levels were significantly higher in BAL from CCSP-p52 mice 48 hours after LPS administration (Fig. 3B). Total inflammatory cell numbers in BAL were also increased in CCSP-p52 mice

compared to WT mice at 48 hours after LPS (Fig. 3C), and this inflammatory infiltrate was characterized by increased numbers of macrophages at 48 and 72 hours and neutrophils at 48 hours (Fig. 3D–F). Nuclear p65, p50, RelB, and c-Rel were assessed by Western blotting of lung nuclear protein from mice 24, 48, and 72 hours after LPS to determine whether altered activation of other NF-κB family members was associated with the enhanced inflammatory influx in CCSP-p52 mice. Compared to WT lungs, no differences in activation of other NF-κB family members in CCSP-p52 lungs were observed at any time point (Fig. 3G, H and data not shown).

Since we observed increased inflammatory cells in BAL from CCSP-p52 mice following LPS treatment, we expected to find increased levels of cytokines/chemokines in the lungs. Therefore, we measured a panel of mediators in BAL fluid at 24 hours after LPS treatment and in lung lysates at 24, 48, and 72 hours after LPS. Surprisingly, no differences were found in levels of G-CSF, IL-1β, MCP-1, MIP-1α, IFNγ, IL-6, or KC between CCSP-p52 and WT mice at any time point (Supplementary Fig. 2A–D). We also measured expression of previously described non-canonical NF-κB signaling targets Cxcl12, Cxcl13, Ccl19, and Ccl21 (4) in lung lysates from CCSP-p52 and WT mice and found no differences between groups (Supplementary Fig. 2E). To determine whether inflammatory cells from CCSP-p52 mice produced more inflammatory cytokines, we isolated macrophage and neutrophil populations from the lungs of WT and CCSP-p52 mice 48 hours after LPS and measured expression of KC, TNF-α, IL-6, and IL-1β by quantitative real-time PCR. However, no increases in cytokine production by inflammatory cells from CCSP-p52 mice were observed (data not shown). Together, these data show that over-expression of p52 in the airway epithelium does not increase cytokine expression in this model.

The p52 precursor p100 preferentially binds to RelB in the cytoplasm, inhibiting its nuclear translocation (17). When non-canonical signaling is activated, processing of p100 to p52 induces translocation of RelB/p52 heterodimers into the nucleus (17, 18). To investigate the effect of RelB over-expression in combination with p52 over-expression on inflammatory cell recruitment, dox-treated WT and CCSP-p52 mice were administered adenoviral RelB (Ad-RelB) or control adenovirus (Ad-Luc) by IT injection. RelB over-expression in the lungs was confirmed by quantitative real-time PCR (Supplementary Fig. 3A), and inflammatory cell recruitment was assessed 96 hours after adenoviral administration. RelB over-expression caused a significant increase in inflammatory cell recruitment, characterized by increased macrophages, lymphocytes, and neutrophils in both WT and CCSP-p52 mice compared to mice treated with Ad-Luc (Supplementary Fig. 3B–E). However, in the context of LPS stimulation, RelB over-expression did not affect inflammatory cell influx into the lungs of CCSP-p52 mice after LPS treatment (Supplementary Fig. 3D,E). Together, these data indicate that RelB over-expression causes an inflammatory response independent of p52. However, RelB over-expression did not augment the effects of p52 over-expression in the context of LPS stimulation, indicating that p52 is the most important component of the non-canonical NF-κB signaling pathway responsible for altering the response to LPS.

To determine whether CCSP-p52 mice are more susceptible to lung injury, we tested their response to a different insult by administering IT bleomycin (0.08 units), a chemotherapeutic agent that causes lung inflammation, injury, and fibrosis in mice. Three

weeks after bleomycin administration, no differences in BAL inflammatory cells or lung fibrosis were observed between dox-treated WT and CCSP-p52 mice (Supplementary Fig. 4), suggesting that p52-mediated exacerbation of lung injury may be dependent on the stimulus.

p52 over-expression causes apoptosis of airway epithelial cells after LPS

Since no differences in cytokine expression were observed between LPS-treated WT and CCSP-p52 mice, we wondered whether p52 over-expression could contribute to lung injury by altering epithelial cell survival. Therefore, we measured apoptosis by TUNEL staining in WT and CCSP-p52 lung sections at 24 and 48 hours after LPS. While no significant differences in apoptosis were observed at 24 hours after LPS, a trend toward increased apoptosis in CCSP-p52 lungs was present at 48 hours after LPS (Fig. 4A). By co-immunofluorescence staining of TUNEL and CCSP, we looked more specifically at apoptosis in the CCSP+ airway epithelial cells where p52 is expressed. At 48 hours after LPS, a significant increase in the number of CCSP+TUNEL+ cells was detected in the airways of CCSP-p52 mice compared to WT mice (Fig. 4B, C). In the absence of LPS stimulation, no significant difference in apoptotic CCSP+ cells was observed in CCSP-p52 mice compared to WT (Fig. 4B). To determine whether apoptosis was restricted to the p52 transgene-expressing CCSP+ airway epithelial cells, we evaluated apoptosis of type II alveolar epithelial cells by co-immunofluorescence staining of TUNEL and the type II cell-specific marker surfactant protein C (SPC). We found no differences in SPC+TUNEL+ type II cells between WT and CCSP-p52 mice after LPS (Fig. 4D). Together, these data suggest that p52 directly regulates epithelial cell survival during conditions of inflammation or cellular stress.

p52 over-expression in stressed epithelial cells leads to enhanced expression of pro-apoptotic factors

To explore the mechanism by which p52 promotes apoptosis of epithelial cells, we generated lung epithelial cells with stable p52 over-expression using the RLE-6TN rat lung epithelial cell line (designated RLE-p52). p52 over-expression and nuclear localization in these cells was confirmed by Western blotting of nuclear protein (Fig. 5A). To investigate whether p52 over-expression resulted in differential apoptosis in RLE-6TN cells, we first tested inflammatory stimuli (LPS, TNF-α, and IL-1β); however, none of these treatments resulted in substantial apoptosis in empty vector control (designated RLE-EV) or p52 over-expressing cells, indicating that these cells are resistant to apoptosis in response to inflammatory stimuli. Next we evaluated the effect of reactive oxygen species stimulation by treating cells with H_2O_2 (100 μM). At 24 hours after H_2O_2 treatment, RLE-p52 cells demonstrated a significant decrease in cell viability compared to RLE-EV cells (Fig. 5B). Increased apoptosis of RLE-p52 cells was supported by Western blotting for cleaved caspase-3 at 18 hours of exposure to H_2O_2 (Fig. 5C).

In another model of acute cellular stress, serum starvation, we found that RLE-p52 cells had significantly reduced cell viability compared to RLE-EV cells as well as the parental cell line (designated RLE-WT) (Fig. 5D). Similar to H_2O_2 treatment, we observed increased apoptosis of RLE-p52 cells by Western blotting for cleaved caspase-3 after 18 hours of

serum starvation (Fig. 5E). To identify specific mediators of apoptosis differentially upregulated in RLE-p52 cells, we measured apoptotic factors in RLE-p52, RLE-EV, and RLE-WT cells after 18 hours of serum starvation using a quantitative real-time PCR apoptosis array. Compared to RLE-EV and RLE-WT cells, ten pro-apoptotic factors were significantly upregulated in RLE-p52 cells, including Bcl10, Bid, Bcl2l11 (Bim), Bok, caspase-4, caspase-6, caspase-7, Fas, Gadd45α, and Pycard (Fig. 6A–J), suggesting that p52 plays a role in regulating expression of these genes in stressed cells and that these genes in turn promote apoptosis.

DISCUSSION

These studies describe the generation of a novel transgenic mouse model that enables expression of the NF-κB family member p52 in specific cell populations and the characterization of the model in airway epithelial cells. Using this model, we have identified an important and unexpected role for p52 in the airway epithelium in the setting of acute lung injury. In CCSP-p52 mice, p52 over-expression did not induce inflammatory cell recruitment or activation of other NF-κB family members. However, in combination with LPS stimulation, p52 over-expression augmented epithelial apoptosis, enhanced lung inflammation without an increase in cytokine production, and enhanced lung injury and mortality. These effects appear to be driven directly by p52, since no changes in other NF-κB family members were observed after LPS stimulation and addition of RelB did not augment the phenotype. In addition, apoptosis of p52-expressing cells was specific to settings of acute cellular stress, since apoptosis was not observed in CCSP-p52 mice without LPS treatment or in RLE-p52 cells under normal culture conditions. In patients with ARDS, increased nuclear p52 staining was observed in the airways and lung parenchyma, suggesting that p52 could impact lung injury. Taken together, our studies implicate p52 as a potential factor in determining ARDS severity through regulation of epithelial survival/apoptosis.

Our findings, in conjunction with studies published by others, suggest that non-canonical and canonical NF-κB activation in the lung epithelium have different effects on inflammatory signaling and inflammatory cell recruitment. Over-expression of constitutively active IκB kinase IKKβ in the lung epithelium drives canonical NF-κB pathway activation causing a profound inflammatory response and elevated chemokine production (6). Here, we show that over-expression of the non-canonical pathway effector p52 does not cause inflammation on its own, but in the setting of LPS treatment can enhance inflammatory cell influx into the lungs, although it is likely that the inflammatory cell infiltrate is an indirect effect of epithelial cell death and altered barrier function. While other studies have suggested that p52 cooperates in regulating inflammatory cytokines in airway epithelial cells (7), we observed no differences in inflammatory cytokine production. In contrast, RelB over-expression led to increased inflammatory cell recruitment, which was not enhanced further by p52 over-expression. However, in the setting of LPS stimulation, we found that RelB over-expression did not augment lung inflammation and injury, indicating that p52 is the functional effector of the non-canonical NF-κB pathway in this model. In a different inflammatory context, RelB has been shown to limit cigarette smoke-induced inflammatory cell recruitment and cytokine production (19). Collectively, these data imply that different

NF-κB pathway components are uniquely involved in regulating lung epithelial inflammatory signaling, and their effects on inflammation may depend on the specific inflammatory signaling environment.

The discovery that p52 over-expression promotes apoptosis of airway epithelial cells after LPS stimulation was unexpected, as many studies have suggested that p52 is pro-survival/proliferation. In fibroblasts, p52 and RelB protect against reactive oxygen species-induced senescence by regulating CDK4 and CDK6 expression and antagonizing p53 function (20), and in prostate cancer cells, p52 promotes proliferation through regulation of cyclin D1 (21). *In vivo* studies have demonstrated that expression of p100 in the mammary gland leads to hyperplasia (22) and global p52 expression caused by deletion of the C-terminal inhibitory domain causes hyperplasia of the gastric epithelium (23). In our studies, we found that p52 promoted epithelial cell apoptosis only in the context of acute cellular stressors, including LPS treatment *in vivo*. In contrast, we observed no differences in bleomycin-induced fibrosis in CCSP-p52 mice. In this model bleomycin causes direct DNA damage leading to cell-cycle arrest and apoptosis of airway and alveolar epithelial cells, followed by inflammation and fibrosis. Although it is possible that apoptosis of CCSP-expressing cells does not impact the degree of bleomycin-induced inflammation and fibrosis, the lack of phenotypic differences between CCSP-p52 mice and WT mice suggests that p52 may have a different functional role in this direct epithelial injury model compared to LPS treatment, which can induce epithelial cell death through extrinsic and intrinsic apoptosis pathways as well as activation of effector cells, particularly neutrophils (24).

Interestingly, of the ten pro-apoptotic genes we identified with increased expression in p52 over-expressing cells during serum starvation, nine are known to be regulated by NF-κB signaling (Bcl2l11, Casp4, Fas, and Pycard) or contain NF-κB consensus sequence binding sites in their promoters (Bcl10, Bid, Bok, Casp7, and Gadd45α), indicating that p52 may preferentially bind these gene promoters under conditions of cellular stress. Structurally, p52 lacks a transactivation domain, suggesting that interactions with other NF-κB family members or transcriptional co-factors are necessary for regulation of target genes. In the setting of cellular stress, the pool of available NF-κB binding partners may be altered or additional transcriptional co-factor(s) that cooperate with p52 may be activated, affecting p52 binding site preferences. Additionally, epigenetic changes may occur as a result of stress signals that alter accessibility of regulatory regions of pro-apoptotic genes. Future studies are necessary to identify factors that modulate the transcriptional outcome of p52 activation in different contexts.

Prior studies have demonstrated that LPS stimulation causes apoptosis of airway epithelial cells in murine models (25, 26), and our studies suggest that p52 augments this apoptotic response. Although we cannot conclude that enhanced epithelial cell apoptosis is directly responsible for increased mortality of CCSP-p52 mice following LPS treatment, epithelial cell apoptosis has been shown to impact the degree of lung injury and survival of rodents after LPS administration (26). Similarly, epithelial cell apoptosis is a prominent feature in the lungs of humans with ARDS (27–31), and the degree of epithelial injury is an important factor predicting patient outcome (30, 32). The identification of increased nuclear p52 in lungs of ARDS patients combined with the effects of p52 expression in the LPS model of

ARDS/acute lung injury indicate that non-canonical NF-κB pathway signaling could be an important factor in regulating epithelial cell survival/apoptosis, barrier integrity, and disease severity in patients with ARDS. Although more investigation is required to better understand the function of p52 in the setting of ARDS, our studies indicate that p52 interactions and/or target genes may serve as potential therapeutic targets for patients with ARDS.

Supplementary Material

Refer to Web version on PubMed Central for supplementary material.

Acknowledgments

We thank the Vanderbilt Transgenic Mouse/Embryonic Stem Cell Shared Resource, supported by NIH grants DK020593 and CA68485, for their technical assistance in generating the CCSP-tTS (tet-O)7-FLAG-p52 transgenic mice and the Vanderbilt University Medical Center Hormone Assay and Analytical Services Core, supported by NIH grants DK059637 and DK020593, for their assistance in running and analyzing the multiplex cytokine bead array.

References

1. Caamaño JH, Rizzo CA, Durham SK, Barton DS, Raventós-Suárez C, Snapper CM, Bravo R. Nuclear Factor (NF)-κB2 (p100/p52) is required for normal splenic microarchitecture and B cell-mediated immune responses. J Exp Med. 1998; 187:185–196. [PubMed: 9432976]
2. Franzoso G, Carlson L, Poljak L, Shores EW, Epstein S, Leonardi A, Grinberg A, Tran T, Scharton-Kersten T, Anver M, Love P, Brown K, Siebenlist U. Mice deficient in nuclear factor (NF)-κB/p52 present with defects in humoral responses, germinal center reactions, and splenic microarchitecture. J Exp Med. 1998; 187:147–159. [PubMed: 9432973]
3. Weih F, Carrasco D, Durham SK, Barton DS, Rizzo CA, Ryseck RP, Lira SA, Bravo R. Multiorgan inflammation and hematopoietic abnormalities in mice with a targeted disruption of RelB, a member of the NF-κB/Rel family. Cell. 1995; 80:331–340. [PubMed: 7834753]
4. Dejardin E, Droin NM, Delhase M, Haas E, Cao Y, Makris C, Li ZW, Karin M, Ware CF, Green DR. The lymphotoxin-β receptor induces different patterns of gene expression via two NF-κB pathways. Immunity. 2002; 17:525–535. [PubMed: 12387745]
5. Weih DS, Yilmaz ZB, Weih F. Essential role of RelB in germinal center and marginal zone formation and proper expression of homing chemokines. J Immunol. 2001; 167:1909–1919. [PubMed: 11489970]
6. Cheng DS, Han W, Chen SM, Sherrill TP, Chont M, Park GY, Sheller JR, Polosukhin VV, Christman JW, Yull FE, Blackwell TS. Airway epithelium controls lung inflammation and injury through the through the NF-κB pathway. J Immunol. 2007; 178:6504–6513. [PubMed: 17475880]
7. Tully JE, Nolin JD, Guala AS, Hoffman SM, Roberson EC, Lahue KG, van der Velden J, Anathy V, Blackwell TS, Janssen-Heininger YMW. Cooperation between classical and alternative NF-κB pathways regulates proinflammatory responses in epithelial cells. Am J Respir Cell Mol Biol. 2012; 47:497–508. [PubMed: 22652196]
8. Zhu Z, Ma B, Homer RJ, Zheng T, Elias JA. Use of the tetracycline-controlled transcriptional silencer (tTS) to eliminate transgene leak in inducible overexpression transgenic mice. J Biol Chem. 2001; 276:25222–25229. [PubMed: 11331286]
9. Tichelaar JW, Lu W, Whitsett JA. Conditional expression of fibroblast growth factor-7 in the developing and mature lung. J Biol Chem. 2000; 275:11858–11864. [PubMed: 10766812]
10. Zaynagetdinov R, Stathopoulos GT, Sherrill TP, Cheng DS, McLoed AG, Ausborn JA, Polosukhin VV, Connelly L, Zhou W, Fingleton B, Peebles RS, Prince LS, Yull FE, Blackwell TS. Epithelial nuclear factor-κB signaling promotes lung carcinogenesis via recruitment of regulatory T lymphocytes. Oncogene. 2011; 31:3164–3176. [PubMed: 22002309]

11. Stathopoulos GT, Sherrill TP, Cheng DS, Scoggins RM, Han W, Polosukhin VV, Connelly L, Yull FE, Fingleton B, Blackwell TS. Epithelial NF-κB activation promotes urethane-induced lung carcinogenesis. Proc Natl Acad Sci U S A. 2007; 104:18514–18519. [PubMed: 18000061]
12. Lawson WE V, Polosukhin V, Stathopoulos GT, Zoia O, Han W, Lane KB, Li B, Donnelly EF, Holburn GE, Lewis KG, Collins RD, Hull WM, Glasser SW, Whitsett JA, Blackwell TS. Increased and prolonged pulmonary fibrosis in surfactant protein C-deficient mice following intratracheal bleomycin. Am J Pathol. 2005; 167:1267–1277. [PubMed: 16251411]
13. Petty JM, Sueblinvong V, Lenox CC, Jones CC, Cosgrove GP, Cool CD, Rai PR, Brown KK, Weiss DJ, Poynter ME, Suratt BT. Pulmonary stromal-derived factor-1 expression and effect on neutrophil recruitment during acute lung injury. J Immunol. 2007; 178:8148–8157. [PubMed: 17548653]
14. Hojgaard A, Close R, Dunn D, Weiss RB, Weis JJ, Weis JH. Altered localization of CXCL13 expressing cells in mice deficient in Pactolus following an inflammatory stimulus. Immunology. 2006; 119:212–223. [PubMed: 16836649]
15. Proietto AI, van Dommelen S, Zhou P, Rizzitelli A, D'Amico A, Steptoe RJ, Naik SH, Lahoud MH, Liu Y, Zheng P, Shortman K, Wu L. Dendritic cells in the thymus contribute to T-regulatory cell induction. Proc Natl Acad Sci U S A. 2008; 105:19869–19874. [PubMed: 19073916]
16. Blackwell TS, Lancaster LH, Blackwell TR, Venkatakrishnan A, Christman JW. Differential NF-κB activation after intratracheal endotoxin. Am J Physiol. 1999; 277:L823–L830. [PubMed: 10516225]
17. Solan NJ, Miyoshi H, Carmona EM, Bren GD, Paya CV. RelB cellular regulation and transcriptional activity are regulated by p100. J Biol Chem. 2002; 277:1405–1418. [PubMed: 11687592]
18. Coope HJ, Atkinson PGP, Huhse B, Belich M, Janzen J, Holman MJ, Klaus GGB, Johnston LH, Ley SC. CD40 regulates the processing of NF-κB2 p100 to p52. EMBO J. 2002; 21:5375–5385. [PubMed: 12374738]
19. McMillan DH, Baglole CJ, Thatcher TH, Maggirwar S, Sime PJ, Phipps RP. Lung-targeted overexpression of the NF-κB member RelB inhibits cigarette smoke-induced inflammation. Am J Pathol. 2011; 179:125–133. [PubMed: 21703398]
20. Iannetti A, Ledoux AC, Tudhope SJ, Sellier H, Zhao B, Mowla S, Moore A, Hummerich H, Gewurz BE, Cockell SJ, Jat PS, Willmore E, Perkins ND. Regulation of p53 and Rb links the alternative NF-κB pathway to EZH2 expression and cell senescence. PLoS Genet. 2014; 10:e1004642. [PubMed: 25255445]
21. Nadiminty N, Chun JY, Lou W, Lin X, Gao AC. NF-κB2/p52 enhances androgen-independent growth of human LNCaP cells via protection from apoptotic cell death and cell cycle arrest induced by androgen-deprivation. Prostate. 2008; 68:1725–1733. [PubMed: 18781579]
22. Connelly L, Robinson-Benion C, Chont M, Saint-Jean L, Li H, Polosukhin VV, Blackwell TS, Yull FE. A transgenic model reveals important roles for the NF-κB alternative pathway (p100/p52) in mammary development and links to tumorigenesis. J Biol Chem. 2007; 282:10028–10035. [PubMed: 17261585]
23. Ishikawa H, Carrasco D, Claudio E, Ryseck RP, Bravo R. Gastric hyperplasia and increased proliferative responses of lymphocytes in mice lacking the COOH-terminal ankyrin domain of NF-κB2. J Exp Med. 1997; 186:999–1014. [PubMed: 9314550]
24. Neff SB, Z'graggen BR, Neff TA, Jamnicki-Abegg M, Suter D, Schimmer RC, Booy C, Joch H, Pasch T, Ward PA, Beck-Schimmer B. Inflammatory response of tracheobronchial epithelial cells to endotoxin. Am J Physiol Lung Cell Mol Physiol. 2006; 290:L86–96. [PubMed: 16100285]
25. Vernooy JH, Dentener MA, van Suylen RJ, Buurman WA, Wouters EF. Intratracheal instillation of lipopolysaccharide in mice induces apoptosis in bronchial epithelial cells: no role for tumor necrosis factor-alpha and infiltrating neutrophils. Am J Respir Cell Mol Biol. 2001; 24:569–576. [PubMed: 11350826]
26. Kawasaki M, Kuwano K, Hagimoto N, Matsuba T, Kunitake R, Tanaka T, Maeyama T, Hara N. Protection from lethal apoptosis in lipopolysaccharide-induced acute lung injury in mice by a caspase inhibitor. Am J Pathol. 2000; 157:597–603. [PubMed: 10934162]

27. Bardales RH, Xie SS, Schaefer RF, Hsu SM. Apoptosis is a major pathway responsible for the resolution of type II pneumocytes in acute lung injury. Am J Pathol. 1996; 149:845–852. [PubMed: 8780388]

28. Guinee D, Fleming M, Hayashi T, Woodward M, Zhang J, Walls J, Koss M, Ferrans V, Travis W. Association of p53 and WAF1 expression with apoptosis in diffuse alveolar damage. Am J Pathol. 1996; 149:531–538. [PubMed: 8701992]

29. Lee KS, Choi YH, Kim YS, Baik SH, Oh YJ, Sheen SS, Park JH, Hwang SC, Park KJ. Evaluation of bronchoalveolar lavage fluid from ARDS patients with regard to apoptosis. Respir Med. 2008; 102:464–469. [PubMed: 17988850]

30. Albertine KH, Soulier MF, Wang Z, Ishizaka A, Hashimoto S, Zimmerman GA, Matthay MA, Ware LB. Fas and Fas ligand are up-regulated in pulmonary edema fluid and lung tissue of patients with acute lung injury and the acute respiratory distress syndrome. Am J Pathol. 2002; 161:1783–1796. [PubMed: 12414525]

31. Galani V, Tatsaki E, Bai M, Kitsoulis P, Lekka M, Nakos G, Kanavaros P. The role of apoptosis in the pathophysiology of Acute Respiratory Distress Syndrome (ARDS): An up-to-date cell-specific review. Pathol Res Pract. 2010; 206:145–150. [PubMed: 20097014]

32. Matthay MA, Wiener-Kronish JP. Intact epithelial barrier function is critical for the resolution of alveolar edema in humans. Am Rev Respir Dis. 1990; 142:1250–1257. [PubMed: 2252240]

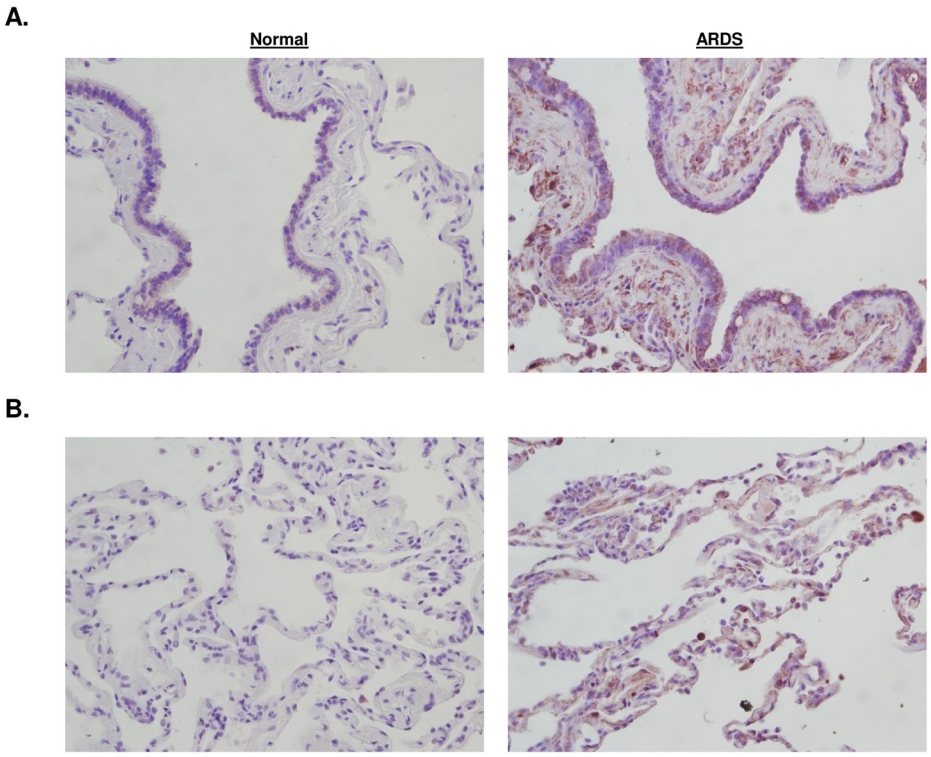

Figure 1.

Increased nuclear p52 staining in airways of ARDS patients. Photomicrographs of p52 immunostaining of airways (A) and lung parenchyma (B) from normal and ARDS human lung sections (40x magnification). Immunostaining is representative of lung sections from 4 individuals per group.

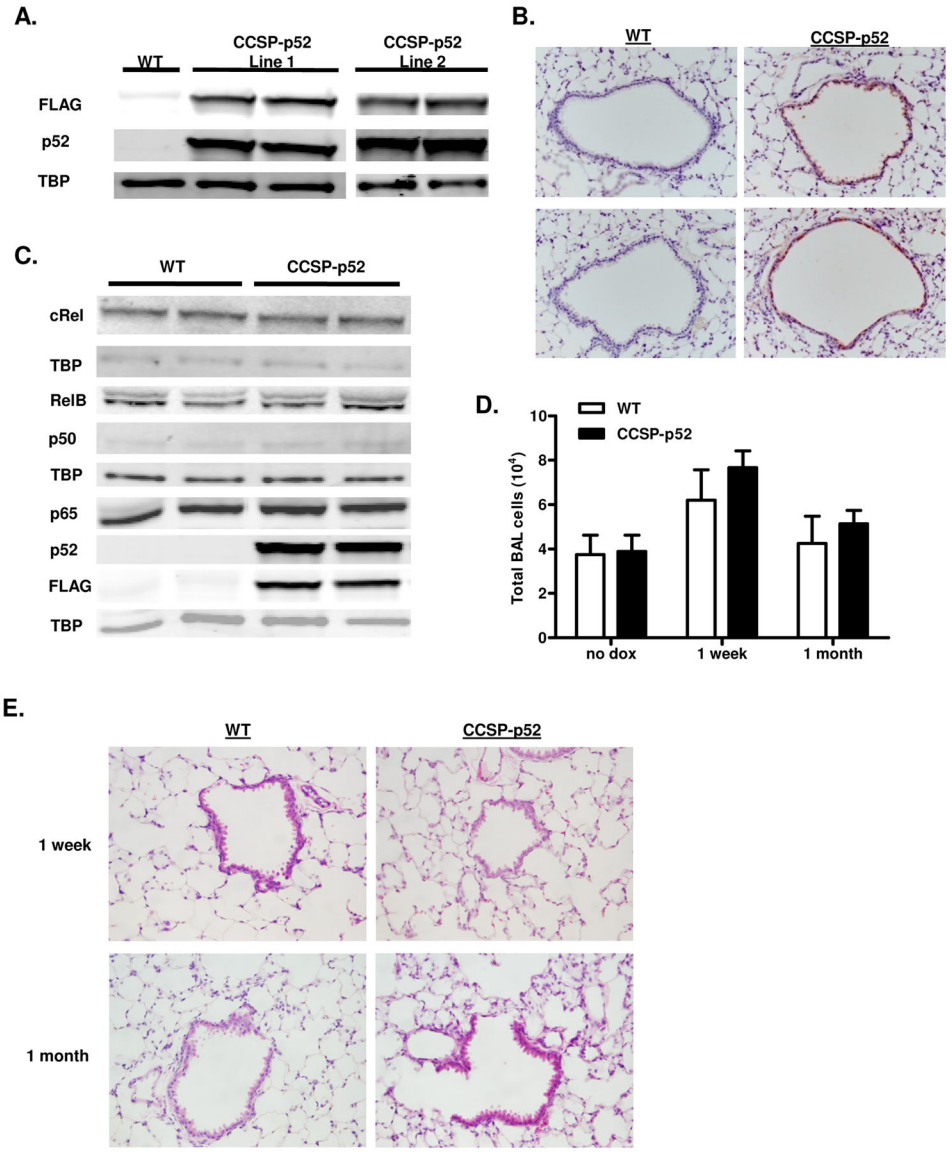

Figure 2.

Characterization of a novel transgenic mouse model of lung epithelial p52 expression. A) Western blot demonstrating FLAG-tagged p52 transgene expression in lung nuclear protein from WT and CCSP-p52 mice on dox for 1 week. B) FLAG immunostaining of lung sections from WT and CCSP-p52 mice on dox for 1 week (20x magnification). C) Western blots for NF-κB family members using lung nuclear protein from mice on dox for 1 week. Three separate Western blots were performed, and TATA Binding Protein (TBP) was probed as a loading control for nuclear protein on each membrane. D) Total BAL inflammatory cell numbers and E) representative lung photomicrographs of H&E-stained lung sections (40x magnification) from WT and CCSP-p52 mice (for no dox and 1 month n=3–7/group, for 1 week n=10–13/group).

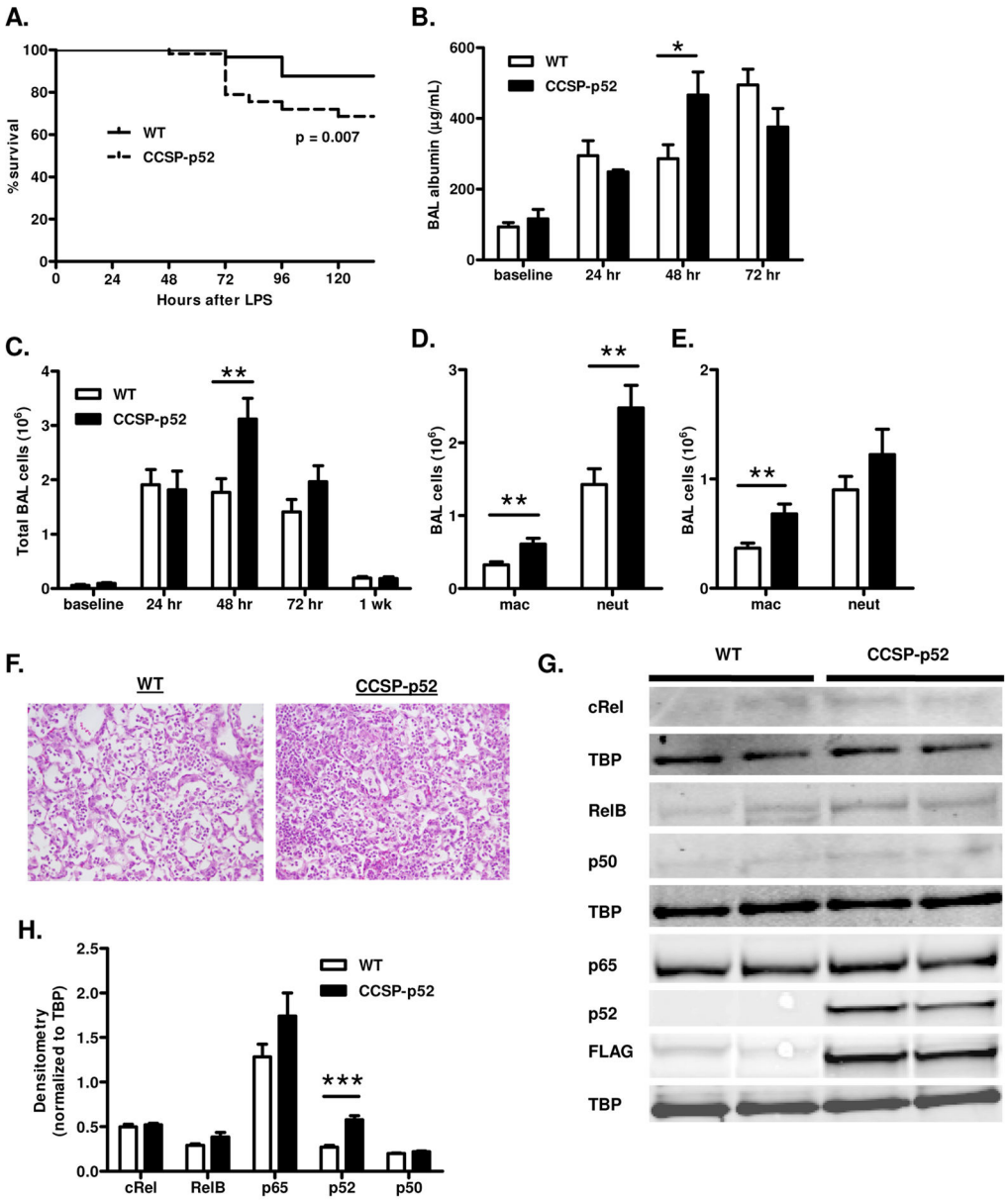

Figure 3.

Treatment of CCSP-p52 mice with LPS results in increased inflammation, lung injury, and mortality. A) Kaplan-Meier survival curve of WT and CCSP-p52 mice after LPS stimulation (n=57–60/group; log-rank test $p<0.01$). B) Albumin measured by ELISA in lavage fluid from WT and CCSP-p52 mice at baseline and after LPS stimulation (for baseline n=4/group, for 24 and 72 hour n=7–8/group, for 48 hour n=12–17/group;*$p<0.05$ compared to WT). C) Total BAL inflammatory cell numbers at baseline and after LPS stimulation (n=10–27/group, **$p<0.01$ compared to WT). BAL inflammatory cell differentials for CCSP-p52 and WT mice 48 hours (D) and 72 hours (E) after LPS (n=12–26/group; **$p<0.01$ compared to WT). F) Representative photomicrographs (40x magnification) of H&E-stained lung sections from WT and CCSP-p52 mice at 48 hours after LPS. G) Western blots and H) densitometry for NF-κB family members using lung nuclear protein from mice at 48 hours

after LPS stimulation. Three separate Western blots were performed, and TBP was probed as a loading control for nuclear protein on each membrane. (***p<0.001 compared to WT).

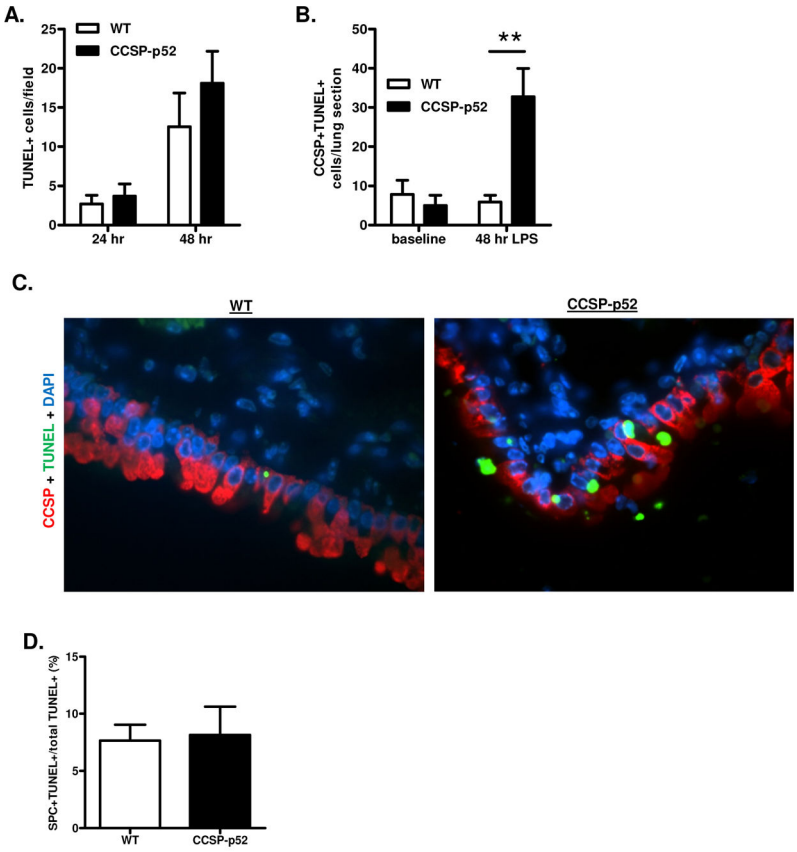

Figure 4.

p52 over-expression causes increased apoptosis of CCSP+ cells after *in vivo* LPS treatment. A) Quantification of TUNEL immunofluorescence staining (average number of TUNEL+ cells per high power field) performed on lung sections from WT and CCSP-p52 mice 24 and 48 hours after LPS (for 24 hours n=3/group, for 48 hours n=6/group). B) Quantification of CCSP+TUNEL+ cells on whole lung sections from WT and CCSP-p52 mice on dox for 1 week (baseline) or 48 hours after LPS (n=5–8/group; **p<0.01). C) Representative confocal images of CCSP and TUNEL co-immunofluorescence staining of WT and CCSP-p52 lungs 48 hours after LPS (red=CCSP, green=TUNEL, blue=DAPI; 60x magnification). D) Quantification of SPC+TUNEL+ cells as a percentage of total TUNEL+ cells counted in ten 20x fields on lung sections from WT and CCSP-p52 mice 48 hours after LPS (n=4/group).

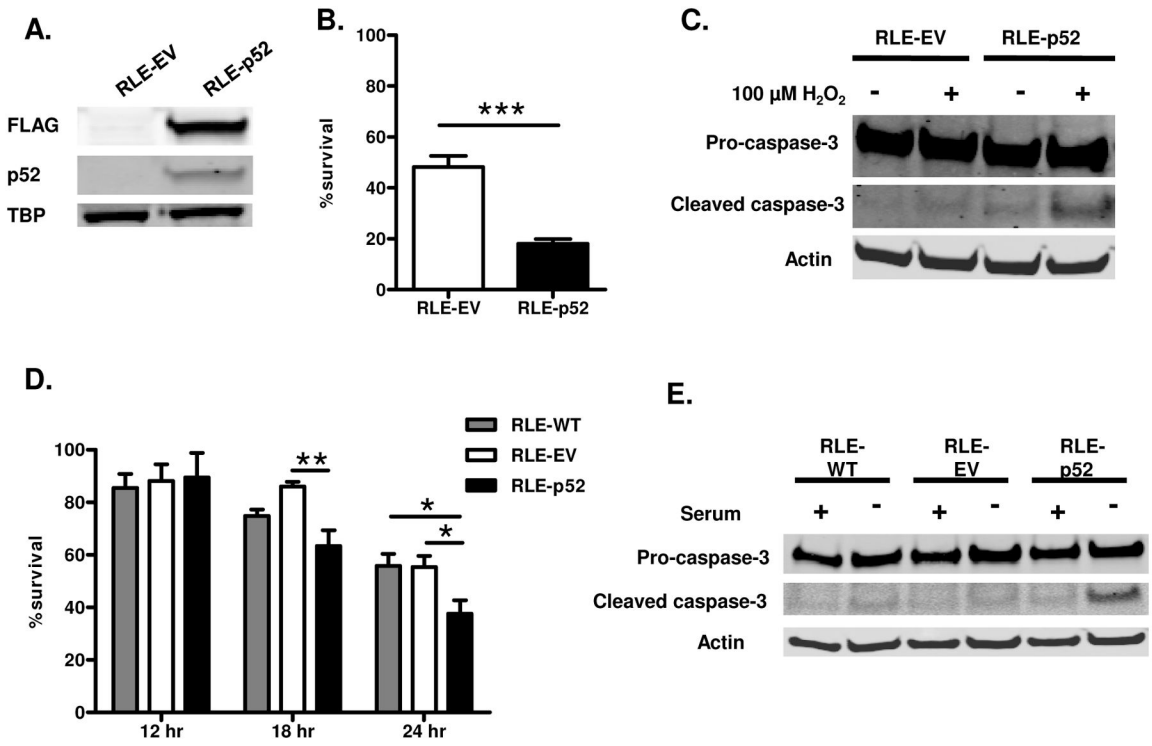

Figure 5.

p52 enhances apoptosis of lung epithelial cells during cellular stress *in vitro*. A) Western blot for p52 and FLAG using nuclear lysates from RLE-6TN cells stably transfected with a p52 expression vector (RLE-p52) or control empty vector (RLE-EV). TBP was used as a loading control. B) Survival of RLE-p52 and RLE-EV cells at 24 hours after H_2O_2 treatment (100 μM) measured by CellTiter-Glo (Promega). Percent survival was determined by normalizing values for each cell line treated with H_2O_2 to untreated values for each cell line (***$p<0.001$ comparing RLE-EV to RLE-p52). C) Pro-caspase-3, cleaved caspase-3, and p52 measured by Western blotting of whole cell lysates from RLE-EV and RLE-p52 with and without H_2O_2 stimulation. Actin was used as a loading control. D) Survival of RLE-p52, RLE-EV, and parental cell line RLE-WT after 12, 18, and 24 hours of serum starvation. Percent survival was determined by normalizing values for each cell line in medium lacking serum to values for each cell line in 10% serum medium at each time point (18 hr **$p<0.01$ comparing RLE-EV to RLE-p52; 24 hr *$p<0.05$ comparing RLE-p52 to RLE-EV and RLE-p52 to RLE-WT). E) Pro-caspase-3 and cleaved caspase-3 measured by Western blotting of whole cell lysates from RLE-WT, RLE-EV, and RLE-p52 cells grown in 10% serum medium or after 18 hours of serum starvation.

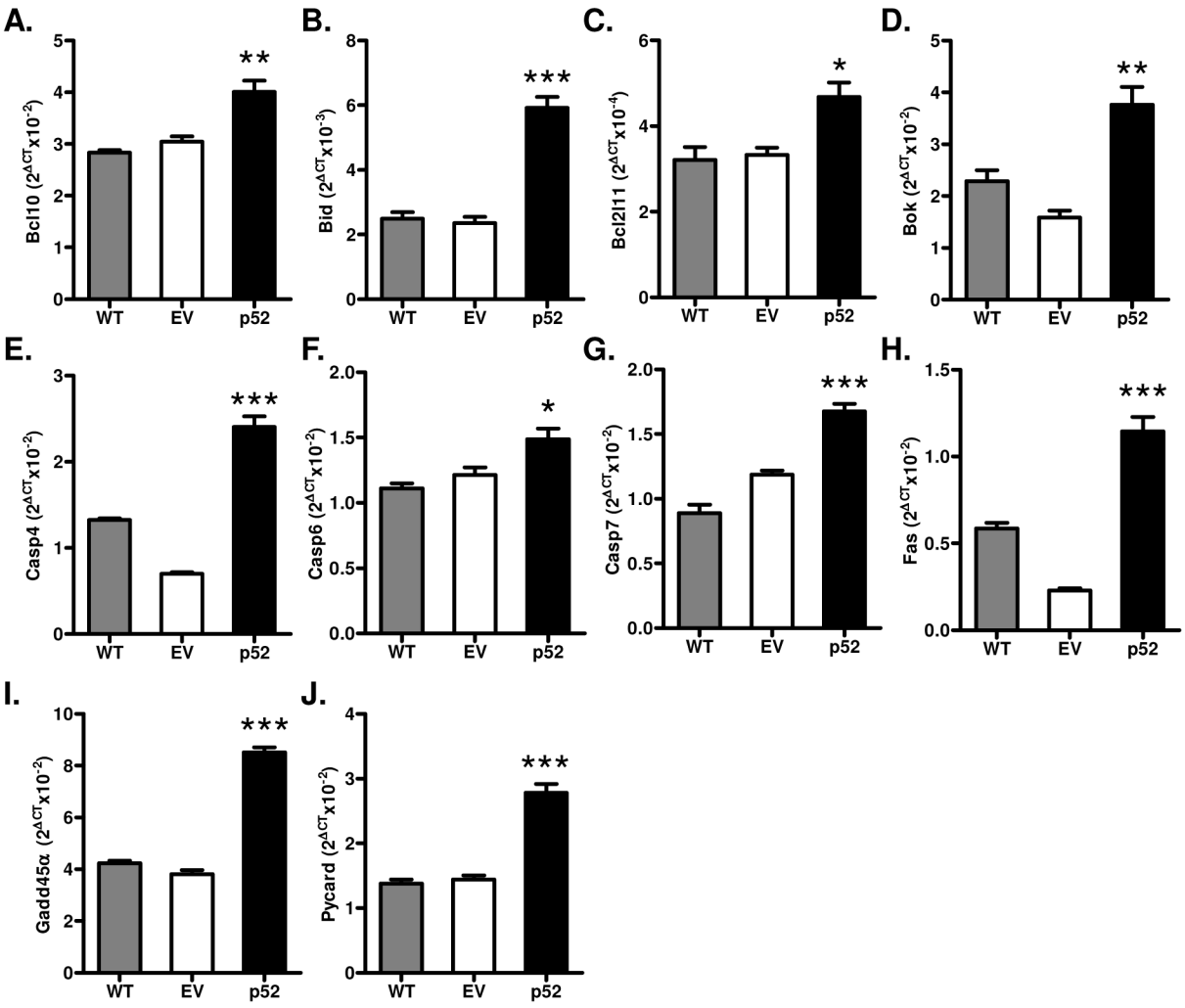

Figure 6.

p52 regulates expression of apoptosis-associated genes during cellular stress. Quantitative real-time PCR analysis of Bcl10 (A), Bid (B), Bcl2l11 (C), Bok (D), Casp4 (E), Casp6 (F), Casp7 (G), Fas (H), Gadd45α (I), and Pycard (J) expression in RLE-WT, RLE-EV, and RLE-p52 cells after 18 hours of serum starvation [n=4 biological replicates/group; (D–M) *p<0.05, **p<0.01, ***p<0.001 comparing p52 to WT and p52 to EV].